HOT WIRE VISUALIZATIONS OF BREAKDOWN TO TURBULENCE IN COMPLEX FLOWS

V.G. Chernoray
Chalmers University of Technology, Applied Mechanics, Göteborg, Sweden

V.V. Kozlov
Institute of Theoretical and Applied Mechanics, Novosibirsk, Russia

L. Löfdahl
Chalmers University of Technology, Applied Mechanics, Göteborg, Sweden

P.R. Pratt
The Queen's University of Belfast, School of Aeronautical Engineering, Belfast, Northern Ireland

The nonlinear stage of breakdown to turbulence is a strongly three-dimensional process and represents a difficult task for experimental studies. Investigation of laminar-turbulent transition in aerospace applications additionally involves a complex base-flow with pressure gradients and secondary velocity components resulting in successive increase of necessary measurements. The developed hot wire visualisation technique offers a possibility for an advanced analysis whilst retaining the advantages of traditional visualisation methods and is especially suitable for resolving such complex flows.

Breakdown in straight and swept wing boundary layers

It is a well-known fact that the surface friction is the main source of drag on aircraft wings, road vehicles and other streamlined bodies. Since the skin friction of turbulent boundary layers is significantly greater than that of laminar boundary flows, it is most important to have an insight into how the laminar-turbulent transition occurs in different three-dimensional (3D) boundary layers. This knowledge would enable prediction and, in a future perspective, also control of all stages of the transition. However, it should be freely admitted that the understanding and control of laminar-turbulent transition in such boundary layer flows have so far remained one of the unsolved problems of fluid dynamics.

Whereas the stability of two-dimensional (2D) boundary layers has extensively been studied theoretically, experimentally and numerically, much less efforts have been devoted to the stability of 3D boundary layer flows due to complexity of phenomena underling the breakdown of laminar flow to turbulent stage [1]. Experiments on swept wing flows have revealed that different transition mechanisms can dominate in a given flow. The main instabilities are viscous, so-called Tollmien–Schlichting (T–S) instability, Görtler instability, cross-flow instability, and attachment-line instability. Although the cross-flow instability is considered to be the most "dangerous" one, our current work is directed toward studies of

the transition caused by the unstable T–S waves, which can be observed in 3D flows with unfavorable pressure gradient.

For 2D wall bounded shear flows two major types of transition are considered. At low level of external perturbations the "classic", T–S transition scenario, is observed, whereas so-called "bypass" transition scenario is associated with rather high level of environmental disturbances. The linear stability theory deals with the prediction whether a given flow is stable or not, and the theory can predict onset of transition and describe the initial linear stage. As far as non-linear wave evolution is concerned, two main regimes of transition have been identified and investigated experimentally. The K-regime, after Klebanoff et al. [2], and the N-regime, experimentally studied for the first time by Novosibirsk group, see Kachanov et al. [3]. In the experimental work [4] it has been shown that both the initial spectral composition of interacting T–S waves and their initial amplitudes predestinate which of these regimes (competing with each other) occurs after the linear stage.

After the pioneer detailed experimental investigation of the K-breakdown scenario by Klebanoff et al. [2], several experimental works and theoretical studies have been conducted to adequately describe this phenomenon, see [5] for review. However, there is still a lack of experiments and computations covering the non-linear evolution of disturbances in 3D boundary layer flows on airfoils at different sweep angles. In order to fill this gap, the generation and evolution of the viscous eigen-waves in 3D swept wing boundary layers have been experimentally studied and some of the results are presented in this paper.

Method of hot-wire visualization

Since the earliest days of fluid mechanics research, flow visualization has been a valuable tool in gaining a qualitative insight into complex flow phenomena. However traditional visualization methods are limited in application and usually give little or no quantitative data. In opposition, a combination of accurate hot wire anemometry techniques and modern data acquisition can be used to perform a "quantitative visualization". This method is especially suitable for studies of three-dimensional transition processes in complex wall-bounded flows. A comprehensive system for automated traversing and data acquisition has been designed and developed for this task at Chalmers University of Technology, and the automation of measurements helps to obtain very extensive velocity data in a short period of time.

Traces within the boundary layer are obtained in a 3D mesh over the surface of the wing. At each point the (phase-locked) traces are sampled and ensemble averaged to give a single period of the oscillation. These are then assembled to form a four-dimensional (4D) spatial and temporal matrix. The waveforms are then separated into the discrete scans of which they consist and in this fashion a number of 3D "frame" matrices are obtained. Isosurfaces of fluctuating velocity are plotted for each frame and displayed in sequence to obtain a dynamic visualization of the process.

Experimental equipment and procedure

The wind tunnel used is located at Chalmers University of Technology. The tunnel is of closed-return type, has a test section 3 m long, 1.8 m wide and 1.2 m high and a maximum velocity of 60 ms^{-1}. The diffuser with contraction ratio of 4.8 is followed by the working section, which has an octagonal cross section with corner fillets. In order to compensate for the growth of the boundary layers, the working section area increases in the streamwise direction by decreasing corner fillets. At the downstream end, ahead of the beginning of the diffuser, a slot establishes a zero pressure difference between the working section and

the surroundings. Moreover, this slot creates a boundary layer suction, preventing separation in the subsequent diffuser. An air cooled electric motor mounted inside the wind tunnel drives a fan, and the cooling air is vented out from the tunnel through channels inside the motor supports. In order to compensate for this cooling flow and for the outflow through the aforementioned slot, a secondary fan provides a boundary layer injection into the diffuser following the motor section. This secondary flow is cooled in order to maintain a constant tunnel temperature. The free-stream turbulence level in the test section is well below 0.1% of U_0 in the velocity range $U_0 = 5$–15 m/s in the frequency range between 0.1 and 10000 Hz. The flow temperature can be controlled with a precision of ±0.1ºC. Velocity in the wind tunnel was monitored using a Pitot–static tube connected to a digital micro-manometer, which also had sensors for temperature and absolute pressure readings. The wind tunnel speed was set at velocity of 12.8 m/s, as in work [5], and corresponding Reynolds number based on the wing chord is about 400000.

The wing model used is of wood construction and has a C-16 aerofoil profile as shown in fig. 1. Wing chord length, C, is 500 mm, span is 1800 mm and the maximum thickness to chord ratio is 0.16 at about 0.3 chord. The top side of the wing after 0.4 chord represents a flat surface thus allowed to study flow without a presence of wall-curvature effects. The wing is mounted horizontally in the middle of the wind tunnel test section, and the mounting mechanism allows to adjust the height of the airfoil location in the tunnel, angle of attack and sweep angle.

A tapping hole is drilled in the wing, in the center of the span at 0.4 chord with the connection located on the lower surface. This tapping is used as a point source to create the disturbance that is studied in the experiment. Periodic blowing and suction is performed by a loudspeaker and harmonic signal is generated by an analogue output board in a computer and amplified. Accurate control of amplitude and frequency is achieved by software. The same board generates the TTL digital signal used for triggering to keep the measurements in phase with the disturbance. The point source frequency was 260 Hz, which gives the reduced frequency, $2\pi f\nu / U_0^{\,2} \times 10^6$, of about 150. The frequency was chosen close to the most amplified frequency of naturally developed disturbances. The amplitude of the point source disturbance was chosen to create rather short linear stage of transition and an extensive nonlinear stage, since nonlinear disturbance development was of a primary interest.

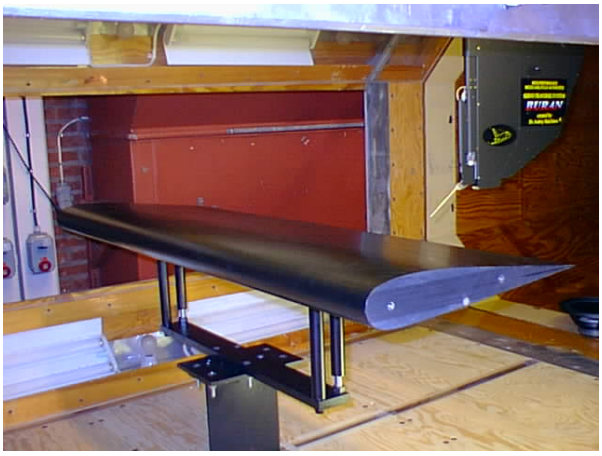

Fig. 1

Measurements are performed by hot-wires and the acquisition system is based on the IO-Tech Wavebook 516 sampling module with expansion unit. This enables 16-bit, 1 MHz, simultaneous sample and hold of 16 analogue channels with full analogue and digital triggering options. Control of the sampling is handled through LabVIEW software.

The software used to control the sampling and save data files is also linked into a program for automated, triggered flow measurements using the traversing system and a predefined mesh of sampling points. This software and traversing system comprise the core of the presented visualization method. The traversing system has been designed and built

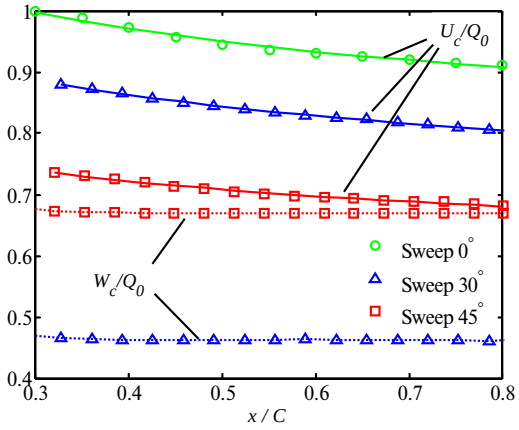

Fig. 2

in house to give the capability of accurate multi-axis placement of flow sensors for use in detailed flow measurements. The system is computer controlled and can be completely automated for long experimental runs through the definition of a geometrical mesh of measurement points. The traversing mechanism is mounted inside the tunnel, on the roof and allow precise positioning of the probe (probes) within the working section. The traverse is driven by servo motors and great care was taken to avoid any mechanical backlash making the achieved positioning accuracy below 10 μm. Traverse motion is controlled from a workstation equipped with a National Instruments Flexmotion board. Motion control software is written using the LabVIEW graphical programming language as well.

After the data had been collected, analysis was carried out in Matlab software package. Voltage traces were converted to velocity traces and phase averaged among 50 realizations to give a single period of the oscillation. These are then assembled to form a four-dimensional spatial and temporal matrix $U(x, y, z, t)$.

Experimental results

The sweep angle configurations under investigation are 0, 30 and 45 degrees. The

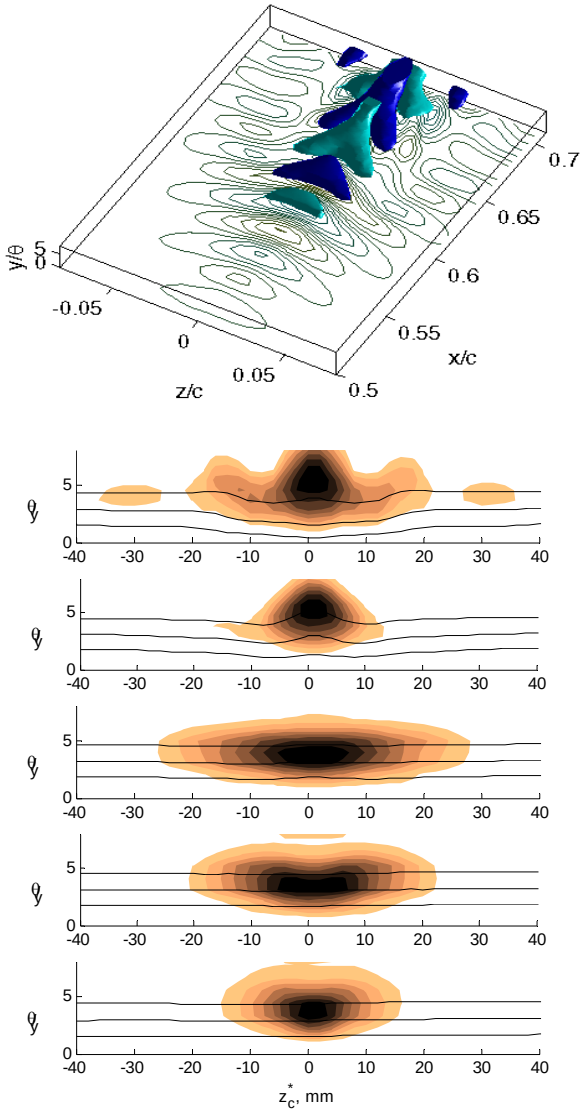

Fig. 3

laminar decelerated flow is created on the upper surface of the airfoil after the point of 0.3 chord. External velocity distribution along the wing chord is shown in fig. 2 for all three configurations of sweep angle. The velocity component U_C is directed perpendicular to the wing leading edge and component W_C is along the leading edge (here index "C" denotes wing-based coordinate system, see [6] for details). Q_0 is absolute value of the free-stream velocity. The crossflow velocity component inside the boundary layer for both

configurations of non-zero sweep was positive and boundary layer profiles resembled corresponding profiles reported in work [6].

Figure 3 shows the development of disturbance from the point source in the case of zero sweep angle (straight wing). Upper part of figure shows isosurfaces of the streamwise velocity disturbance, where blue and light-blue colours represent positive and negative values of the disturbance amplitude respectively. Bottom part of figure shows disturbance r.m.s. (shading) at levels of 10, 20… 90% of local maximum and contours of mean streamwise velocity (levels of 25, 50 and 75%) for streamwise positions, x/C, of 0.48, 0.54, 0.6, 0.66 and 0.72, which are shown increasing from bottom to top. In figure the spanwise and streamwise coordinates are scaled by the wing chord, C, and the wall-normal coordinate is scaled by the boundary layer momentum thickness, θ.

Figures 4 and 5 depict measured point-source disturbance for the configurations of 30 and 45º sweep angles respectively. The measured quantities are shown as in fig. 3 and streamwise positions for given (y, z) contour slices are same as in fig. 3 as well. It can be noted that depicted velocity component is streamwise velocity in the wind-tunnel related coordinate system. Coordinate z_C * is spanwise coordinate, which is shifted so that its origin is in-line with the blowing-suction hole, see [6] for details.

As can be noted from results of fig. 3, in the case of zero sweep angle a typical curved, symmetrical wave front is seen developing from the point source. Spectral analysis was performed, which showed that until 0.55 chord the disturbance development is linear and interactions with the mean flow do not occur. The most amplified are spanwise modes with the spanwise wavenumber, β, equal to 0 degrees, and the three-dimensional shape of the generated wave-train is owing to the flow receptivity mechanisms which are responsible for the initial shape of the

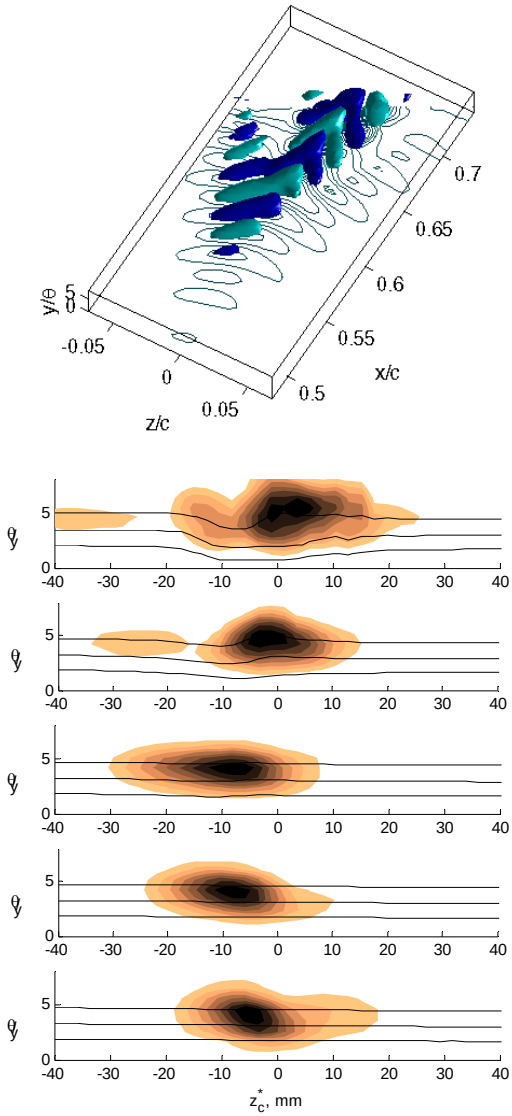

Fig. 4

shape of the perturbation generated near the source. Further downstream, as the disturbance magnitude grows, the wave structures are getting distorted and Λ-shaped vortices are formed. The nonlinear events are revealed as appearance of consequent superharmonics of main frequency, which is a characteristic feature of the K-type breakdown. Detailed modal analysis of the disturbance and analysis of the disturbance random counterpart resembles the behaviour of corresponding quantities in a flat plate boundary layer breakdown [7]. The amplification rates of the modes are higher due to the action of unfavourable pressure gradient.

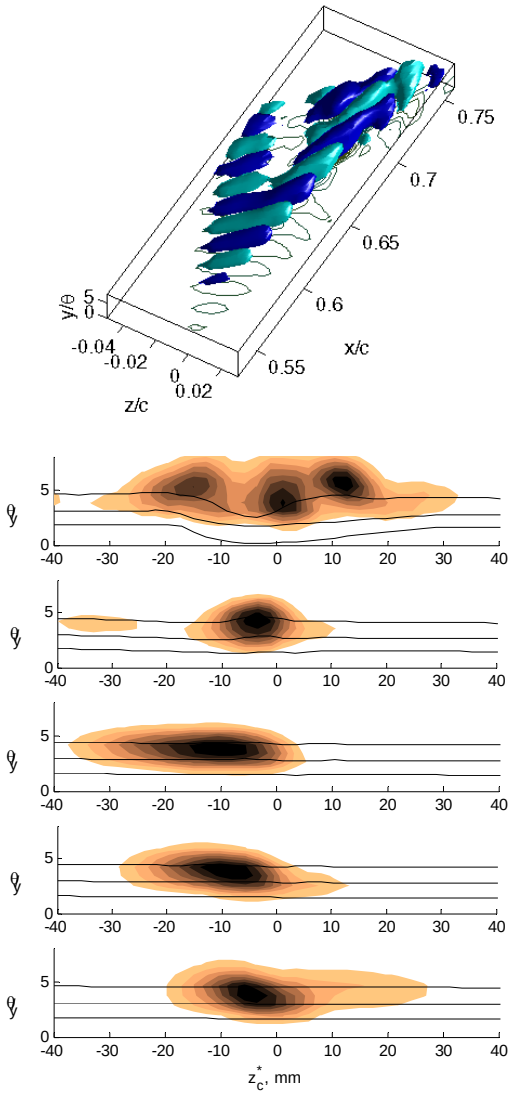

Fig. 5

The presence of (spanwise) crossflow velocity component changes the breakdown process for the configurations of 30 and 45° sweep. In both these cases, as in the case of straight wing, T–S type instabilities dominate at the initial stage of breakdown, which means that the most amplified are modes parallel to the model leading edge ($\beta = -30°$ and $\beta = -45°$ respectively). Modal decomposition of perturbations additionally showed that disturbances excited by the point source are rather similar in all three cases very close to the source and the wave-trains are developed in different way mostly due to the mentioned difference in modal amplification. Furthermore, one can observe from figs. 4 and 5 that the wave-train perturbations start intensively interact with the mean flow after position x/C=0.6. The process takes place, which is similar to process observed in ref. [8], namely, the nonlinear interaction lead to the gradual distortion of the flow structures according to the shape of the three-dimensional base-velocity profile. In addition, downstream of this position another modes, the so-called crossflow modes, start to dominate and these modes are angled approximately perpendicular to the T–S modes. The complex action of these two factors leads to the formation of unsymmetrical structures and changes the nonlinear stage of the flow breakdown dramatically.

References

[1] Reed H.L., Saric W.S. Stability of three-dimensional boundary layers, *Annu. Rev. Fluid. Mech*, 1989, Vol. 21, pp. 235–284.

[2] Klebanoff P.S., Tidstrom K.D., Sargent L. M. The three-dimensional nature of boundary layer instability, *J. Fluid Mech.*, 1962, Vol. 12, pp. 1–34.

[3] Kachanov Y.S., Kozlov V.V., Levchenko V.Y. Nonlinear development of a wave in a boundary layer, *Izv. Akad. Nauk SSSR, Mekh. Zhidk. Gaza*, 1977, Vol. 5, pp. 85-94 (in Russian). Transl. *Fluid. Dyn.*, Vol. 12 (1978), pp. 383–390.

[4] Saric W., Kozlov V., Levchenko V. Forsed and unforced subharmonic resonance in boundary layer transition, *AIAA Paper* No. 84-0007, 1984.

[5] Chernoray V.G., Bakchinov A.A., Kozlov V.V., Löfdahl L. Experimental study of the K-regime of breakdown in straight and swept wing boundary layers, *Physics of Fluids*, 2001, Vol. 13, No 7, pp. 2129-2132.

[6] Chernoray V.G., Dovgal A.V., Kozlov V.V., Löfdahl L. Experiments on secondary instability of streamwise vortices in a swept wing boundary layer, *J. Fluid Mech.*, 2005, Vol. 534, pp. 295-325.

[7] Bake S., Meyer D.G.W., Rist U. Turbulence mechanism in Klebanoff transition: a quantitative comparison of experiment and direct numerical simulation. *J. Fluid Mech.*, 2002, Vol. 459, pp. 217-243.

[8] Litvinenko Yu.A., Grek G.R., Kozlov V.V., Löfdahl L., Chernoray V.G. An experimental study of varicose instability of streaky structure in a boundary layer of swept wing, *J. Thermophysics and Aeromechanics*, 2004, Vol. 11, No 1, pp. 1-11.